Deep Learning Segmentation of Nuclei Cells in divergent images

Johana M. Ramirez Borda
Universidad de los Andes
jm.ramirez11@uniandes.edu.co

Francisco A. Rozo Forero
Universidad de los Andes
fa.rozo1843@uniandes.edu.co

G. A. Espinosa
Universidad de los Andes
g-espino@uniandes.edu.co

1. Introduction

Pathology is the study of the cell morphology that is performed when a tissue sample is removed from the body. Annually, more than 500 million of pathology tests are conducted and they play a crucial role in more than 70% of medical diagnoses. Therefore, these test are considered as the "gold standard" when diagnosing and finding the cure of the majority of diseases, including cancers, metabolic disorders and even psychiatric diseases. Likewise, the pathologist plays an important role since, using the tests results, informs about the clinical decisions related to patient treatment. However, analyzing numerous biopsy slides represents an intensive and time consuming labor [7],[18],[11],[12].

For that reason, digital pathology and computarized approaches to analyze microscopy images have played a significant role in the last years. These methods allow faster and reproducible analysis, which leads to better, faster and more accurate results. In addition, this new approach not only benefits pahtologists in their daily labor, but patients who will have a quantitative diagnosis, a personalized treatment and help in disease progression evaluation [[7],[18],[11],[12]].

One of the most common and difficult tasks when studying pathological images, is the automated nuclei detection and segmentation. In fact, this task is a prerequisite in computer-aided diagnosis and is considered as the basis of automated medical image analysis. Even more, nuclei detection supports the analysis of morphological tasks such as calculating the size, texture and shape of the cell, and also, it can lead to information about presence of disease and its progress [[7],[18],[11],[12]].

In addition, according with the Broad Institute of Harvard and MIT, one of the major problems in the search for effective medicines is finding cell nuclei in microscopy images. This due to the fact that, when trying to discover a good drug, it's neccesary to detect and analyze cell changes and usually, the first step in this process is to identify nuclei [3]. However, the high variability in images because of differences in slide preparation, image acquisition and nuclei heterogeneity makes the automatic nuclei segmentation a difficult problem [11].

As a result of this problems, the Broad Institution is the data partner for the Data Science Bowl this year, which is presented by Booz Allen Hamilton and Kaggle. They decided that the purpose of the 2018 Data Science Bowl is to find the nuclei in divergent images to advance medical discovery. Therefore, seeking to contribute to this need, both the objective and the database to be used in this project will be those provided by them on the Kaggle website [9].

Actually, investigators struggle while analyzing effects of chemicals in cells because it takes too much time looking at all the images. In consequence, more time is spent in the research and more money is required to keep the projects ongoing. Therefore, allowing investigators to skip tasks of recognition in large databases of images can improve the speed and quality of investigations. Also, it can reduce financiering costs while providing better results [9].

Cells are the smallest structure that composes every living organism and is the main base of life. Inside the cells, there is a nucleus which is the main organelle of the eukaryotic cells, because it contains most of the genetic material. The main functions of the nucleus include storing of DNA, replication of it and synthesis of ribosomes. Hence, fast detection of nucleus in cells improves drug production, detection of pathologies and development of cures to it [15].

Analyzing small structures like cells and their nucleus, requires high resolution microscopes to gather high quality images. Also, lot of images can be easily recollected and stored for further analysis. However, the microscopes cant provide any valuable information about the status of cells per se. To do so, experts must check these images by observing them and concluding about them; or in a better scenario, image processing and computational software can perform more efficiently [3].

Most of the time, effective strategies to identify specific diseases, begin with the identification of the nucleus inside of a cell. Nuclei identification can be difficult because it not always has a typical form. Also, two or more cells can overlap, making it difficult to detect each nuclei separately. Finally, the imaging techniques used to acquire the images

may vary within investigations, which leads to a need of an algorithm that identifies the nuclei regardless of the technique used [3].

2. Related work

Through history there have been tested numerous methods in order to segmentate cells nuclei. In this section, the following methods, as well as its advantages and disadvantages, are going to be presented in order to contextualize and lead up our methodology: thresholding, morphology, HAT, LoG, watershed, K-means, Graph cuts and deep learning.

2.1. Thresholding

One first approach that has been used when segmenting nuclei of cells is based on thresholding. In this method, all pixels whose intensity is above some threshold are assigned to the value one, or cero in the opposite case. However, thresholding can be a successful method just when cells are isolated, on the contrary, for overlapping objects, this method is not good enough. Therefore, thresholding is usually used as a process that facilitates or precedes actual segmentation [7].

2.2. Morphology

One second approach is based on morphology. Its main idea is to probe the image with a structuring element and analyze how this shape fits or misses the shapes in the image. There are two basic operators in morphology called erosion and dilation. The first one shrinks the boundaries of foreground pixels, and the second one enlarges them. Also, based on these two operators, there are opening and closing. Opening is the process of developing an erosion followed by a dilation, it is useful when eliminating small objects and sharpening peaks. Closing is the opposite process (dilation and erosion) and it fuses narrow breaks and it fills small holes. In addition, the morphological gradient helps in edge detection, which can be useful when segmenting [7].
Within the family of methods that use morphology it is found the one called Ultimate erosion (UE) and is commonly used for marker detection. In this method, starting with a binary or thresholdized image, for each non-convex component, it is applied iteratively an erosion until one more erosion will remove that component, or until that component is convex. One of the advantages of UE is that overlapping objects can be separated, however, it can produce more than one marker within a cell [18].

Another method that uses morphology was implemented by Yang et al. [18] to detect nucleus markers through conditional erosion (CE). Their methodology is based on the use of four 7x7 masks for coarse erosion (which will preserve shapes of cells), two 3x3 masks for fine erosion (that will avoid under-segmentation) and two thresholds T1 and T2. First, they erode iteratively with the coarse structures until the size of the component is smaller than T1, then, they erode with fine structures until the size of the component is smaller than T2. The results are collected as markers. Similarly to UE, CE is defined on binary images and it also requires two more parameters (T1 and T2) that have to be carefully selected [18].

2.3. H-maxima Transform (HAT)

Unlike the methods previously mentioned, this one is usually performed in original intensity images. Raimondo et al. [14] have proposed a new approach based on HAT in order to detect nuclei on fluorescence in situ hybridization (FISH) images. H-maxima transform suppresses the regional maxima whose height is not larger than h. Their methodology starts with normalizing intensity by its maximum pixel value in the B channel of RGB space. Then, they perform top-hat filtering to reduce the effects of color diffusion and segment out the foreground trough Otsus method. Later, they identify and fill the holes within a nucleus and finally they apply HAT to marker selection. These methods require predefined value of h, which is not easy to find in real applications [7],[18].

2.4. Blob detection: Laplacian of Gaussian

When analyzing medical images, LoG filter is one of the first and also most common method used to detect small, blob objects such as nuclei or cells in microscopy images. Moreover, it is useful when detecting regions in the image that are brighter or lighter than the surrounding [7].

In this method, the first step is to convolve the image with a Gaussian kernel in order to smooth and attenuate noise. This convolution is made at a certain level t that is related with the radius of the blobs: $r = \sqrt{2t}$. Then, the Laplacian operator is applied to the Gaussian representation of the image. In this sense, once smoothed, the Laplacian will highlight regions of rapid intensity change like edges. However, a common problem with LoG method is that the operator is dependent on the relationship between the size of the blob object and the size of the Gaussian kernel used. Therefore, if one wants to automatically detect objects of different or unknown size, it is necessary to use a multi-scale approach [10], [1].

2.5. Watershed

This method is one of the most popular when segmenting overlapping cell nuclei. It is commonly used in grayscale images, gradient images and complemented distance images. It usually starts with a group of markers (pixels) and it gradually floods the surrounding regions of markers (catchment basins). These catchment basins are separated from others by maximum altitude lines (watershed lines). With this method, it is possible to classify every pixel as either

belonging to the catchment basin, associated with one of the local minima, or to the watershed line. Finally, although this approach is simple, it often leads to over-segmentation and therefore it is usually needed a post-processing step [7], [8], [1].

2.6. K-means

Chi Liu et al.[11] proposed that the basic idea of detection is to find local evidence for the presence or absence of a nucleus in the image. Therefore, in their methodology they created a filter bank composed of rings of different sizes. The maximum and minimum radius were estimated given prior information obtained from the dataset. In the response map, pixels having ring-shaped surrounding with radius similar to that of the filter will produce strong responses and will be considered as likely to be nucleus centers. On the contrary, other type of tissue structures, or noise, will have weak responses. In this sense, in order to detect cell nuclei, k-means clustering method is used to classify responses into three possible categories: background, nonnuclei structures (weak responses) and potential nuclei (strong responses). Then, using connected component analysis, nuclei seeds can be obtained by computing the mass center of each cluster within those of strong responses [7], [17].

2.7. Graph-cuts

This method represents an image as a weighted graph were all the pixels (nodes) are related to other pixels with weights (edges). Every pixel is compared to every other pixel and the weight of their affinity is expressed as a number given by the similarity measure of any of their characteristics. The graph-cuts method partition the graph into subgraphs whose similarity is high within them. The dissimilarity between two subgraphs A and B can be represented as the sum of the edges that separate them that must be removed. This total weight is called a cut. The place where the cut takes place based on a threshold. The normalized cuts method solve this problem by optimize the cut(s) based on a generalized eigenvalue [7],[1].

2.8. DL(Deep learning)

Unlike those methods that require hand-crafted features for object classification, CNN (convolutional neural networks) automatically learn multi-level features which preserves relevant information and are irrelevant to variations of samples [19].

Ciregan et al. [19] applied a deep CNN to detect mitotic cells in breast cancer histology images. This CNN provided a probability for a given centroid of a mitotic cell in the form of a map. Then, this map was smoothed with a disk kernel and, using the algorithm of non-maxima suppression, the final centroids were detected [19]. Moreover, Cui et. al [5]proposed a end-to-end deep neural network in order to segmentate individual nuclei.

Another example of the many studies in this field uses the DL(Deep Learning) of Convolutional Neural Network for Nuclei Cells. It includes a selection of the VOI(volume of interest) which is essential to segmentate the actual Neuronal nuclei cells of interest. The DL process was used with a data set of Micro-CT Images of the Brain. The results showed fact-based 3D Solid models of neuronal nuclei cells. This allowed an approximate construction of solid NURBS meshes for patient-specific brain nuclei cells, geometric models for PDE-IGA and a computerized axial tomography imaging reconstruction [6], [4].

Finally, the math segmentation approach is usually achieved using canny and otsu commands from Matlab and python functions for DL(DeepLearning). In this sense, math application of the DL segmentation is based on the study of the basic functions of Splines, Bezier Curves, and the B-Splines [13], [16].

3. Database

3.1. Images

The database was provided by Booze Allen Hamilton via *kaggle.com*[2]. It contains 265 images of one or more cells with their nuclei visible taken with three different techniques, where 200 correspond to the train set while 65 to the test set. The first technique contains 185 images where the background is black, cells have a gray tone and their nuclei is white (see figure 1). Finally, the last technique holds 15 images in the train set, whose background is light gray, the cells are darker gray with their nuclei being almost black (see figure 2).
Each image has a different amount of cells in it; those with the least contain four while some of them have more than twenty. Also, some have nuclei that are close to each other, making it difficult to differentiate one from each other.

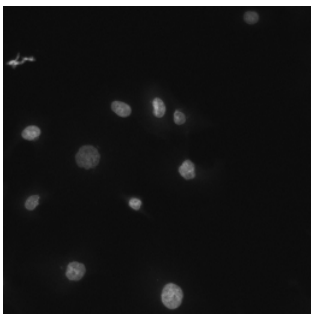

Figure 1. Class 1 image in database

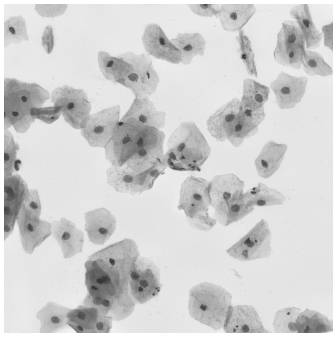

Figure 2. Class 2 image in database

3.2. Annotations

Each image has its own *n* number of annotations, where each one of them is a black & white image where the white region corresponds to a single nuclei segmentation(see figure 4).

Figure 3. Annotation for one nucleus.

If all the annotation images are summed into one, the resultant image will contain all the segmented nuclei (see figure 5).

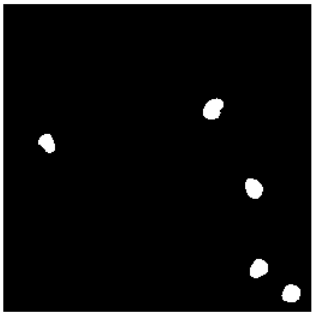

Figure 4. Complete segmentated nuclei annotation.

3.3. Evaluation Methodology

To evaluate the performance of the algorithm, the jaccard index must be implemented. As each image requires its nuclei to be segmentated in their correct location, the jaccard index allow to evaluate the similarity between the annotations and the predictions with a numerical value between 0 and 1. It compares the matching pixels and mismatching pixels of both images with the following equation:

$$J = \frac{A \cap B}{A \cup B} \tag{1}$$

4. Methodology

In the first place, the most basic approach was implemented: thresholding. To do so, the RGB image was converted to gray-scale and then the Otsu's method was used in order to compute a threshold that will allow the image to have logical values. Zero (0) corresponds to non-nuclei region and one (1) corresponds to nuclei region. This was possible using the function *graythresh* of MATLAB, which chooses the threshold that minimize the intraclass variance of the thresholded black and white pixels. An example of an original image and its binary version is shown in Figure 5 for Class 1 images and Figure 6 for Class 2 images.

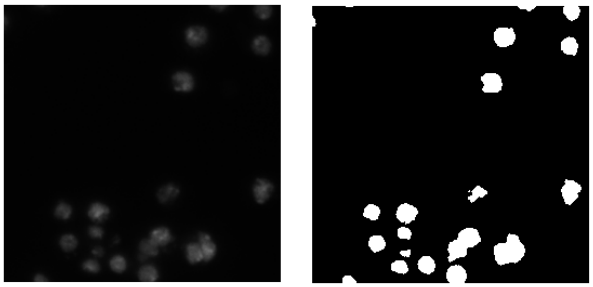

Figure 5. Original Class 1 RGB image and its binary version

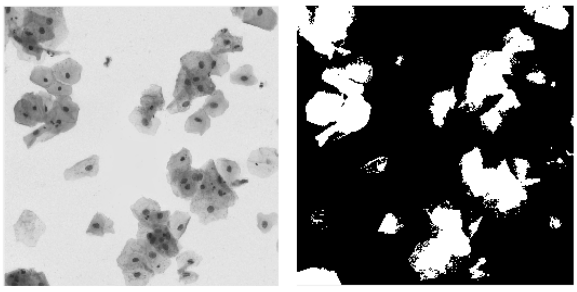

Figure 6. Original Class 2 RGB image and its binary version

The first Jaccard index was calculated, for both classes, between the binary image and its annotation and the results is shown in Table 1 and Table 5.

Second, once obtained the binary version, the morphological operations of erosion, dilation, closure and opening were applied to them in order to assess if the segmentation

results improved using these methodologies. To do so, a disk was used as structuring element and its radius was varied between 1 to 3 for Class 1 and between 1 to 25 for Class 2. The values of the radius were selected based on the results shown in Figures 5 and 6. For example, whereas in class 1 the thresholded image detected smaller and circular-shape forms, class 2 resulted in bigger and amorphous figures. Therefore, in order to get to small detections for nuclei cells in class 2, we had to use structuring elements with bigger radius to decrease noise. Moreover, the Jaccard indexes obtained in each case are shown in Table 1 and Table 5.

Third, in order to test other methods, k-means was also used to divide pixels between nuclei and non-nuclei. To do so, three values of possible number of clusters were tested in class 1: 2, 3 and 4 and six different values for class 2: 2, 3, 4, 5, 6, 7. Therefore, the Jaccard index obtained in each case is shown in Table 2. Then, once calculated the best result of k-means, the same morphological operations were applied to this resulted image. The Jaccard indexes obtained are shown in the Table 3.

Finally, watersheds was tested by applying the technique of minima imposition. To do so, three values of flooding height were used: 3, 5 and 10. However, the obtained results were not as good as those obtained before (see Table 4).

5. Results and discussion

5.1. Class 1

First, the images were thresholded with their respective value obtained with the Otsu's method, having an average jaccard index of 0.6975 (see Table 1). Then, to improve the results, morphological operations such as dilation, erotion, closure and opening were applied to the binary images to see which was the most useful. As seen in table 1, the best results where for dilation after thresholding, which means that nuclei region is not segmented after it. This is also reflected with the Jaccard indices obtained when eroding the images, which get significantly reduced. Also, closure has better results than opening, as closure fill holes and connect close elements. Finally, for this class, thresholding has a good performance because cell nuclei from the cells have a gray tone that is different from the black background and there are no other visible organelles.

Table 1. Jaccard index obtained when thresholding class 1 images, using otsu and then applying the most important morphological operations to the resulted image.

Method	Radius of the structuring element (disk)	Jaccard
Thresholding	-	0.6975
Erosion	r = 1	0.5748
	r = 2	0.4484
	r = 3	0.3214
Dilation	r = 1	0.7806
	r = 2	0.7920
	r = 3	0.7313
Closure	r = 1	0.6980
	r = 2	0.6989
	r = 3	0.7026
	r = 4	0.7015
Opening	r = 1	0.6951
	r = 2	0.6866
	r = 3	0.6636

Table 2. Selection of number of clusters in k-means that improved the Jaccard index in class 1 images

Method	Number of clusters	Jaccard
k-means	k = 2	0.7955
	k = 3	0.7934
	k = 4	0.7888

These values of number of clusters were selected based on the idea that class 1 images didn't present much noise and the nuclei was already defined. In fact, this idea can be represented in Table 2, where even with a small value of k, the Jaccard index obtained was higher than those obtained with class 2 images (see Table 6).

Table 3. Jaccard index obtained when using the best result of k-means in class 1 images and then applying to it the most important morphological operations.

Method	Parameter	Jaccard
k-means	k=3	0.7955
Erosion	r = 1	0.7056
	r = 2	0.5884
	r = 3	0.4546
Dilation	r = 1	0.8091
	r = 2	0.7539
	r = 3	0.6536
Closure	r = 1	0.7946
	r = 2	0.7927
	r = 3	0.7900
Opening	r = 1	0.7934
	r = 2	0.7888
	r = 3	0.7867

In table 3 is shown that kmeans clustering for class 1 had

an overall performance better than the otsu's thresholding. Also, dilation and closure kept being better than erosion and opening. For this method, the color data was used without *xy* position coordinates, because, as mentioned before, nuclei cells have different tone than the background, which makes it useful to separate the nuclei in the image regardless of their position.

Table 4. Jaccard indexes obtained using watersheds in class 1 images

Method	Parameter	Jaccard
Watersheds	h = 3	0.4311
	h = 5	0.4878
	h = 10	0.4767

When extending regional minimums, low values had to be used because the low grayscale tones in the images. Moreover, it oversegmentated the image, so closure had to be used to remove those boundaries that fragmented the nuclei. Yet, it had an overall low performance and didn't segmented some nuclei from each image, having the best jaccard index value of 0.4878 (see table 4).

In short, after all this process, the best nuclei cell segmentation achieved in class 1 images resulted in a Jaccard index of 0.8091 and is shown in Figure 7.

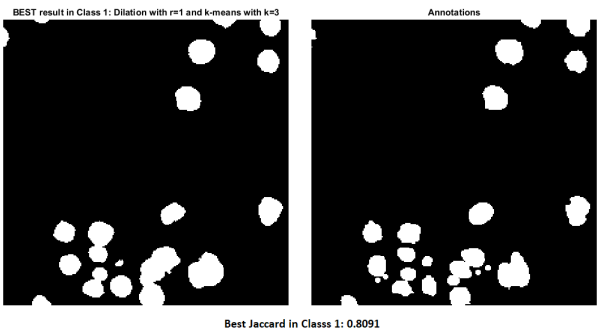

Figure 7. Best nuclei segmentation in class 1 images.

5.2. Class 2

Table 5. Jaccard index obtained when thresholding class 2 images, using otsu and then applying the most important morphological operations to the resulted image.

Method	Radius of the structuring element (disk)	Jaccard
Thresholding	-	0.1096
Erosion	r = 5	0.1322
	r = 10	0.1384
	r = 20	0.1439
	r = 25	0.1353
Dilation	r = 1	0.1012
	r = 5	0.0814
Closure	r = 3	0.1041
	r =5	0.1011
	r = 10	0.0946
Opening	r = 5	0.1192
	r = 10	0.1180
	r = 15	0.1048

Otsu's method and kmeans were implemented as well in the class 2 images. However, the results were notoriously less efficient than in the class 1. Unlike it, class 2 images got low Jaccard index when thresholding. First, due to the fact that, dissimilar to class 1, the nucleus of class 2 presented a bigger variety of gray tones. Therefore, when thresholding with a low value, many false negatives were going to be detected. On the contrary, when using a higher threshold less false positives will be detected at a cost of less true positives detected. This happens because some cells overlap each other, creating a darker area in the image that acquire a similar or darker tone than the nucleus of some cells. The more cells that overlap, the darker the region is. Moreover, some cells are further than others and look more transparent, so their nucleus had a lighter tone that makes them likely to be classified as background.

Table 6. Jaccard indexes obtained when varying the number of clusters in k-means in class 2 images.

Method	Number of clusters	Jaccard
Kmeans	k = 2	0.0998
	k = 3	0.2320
	k = 4	0.4527
	k = 5	0.5263
	k = 6	0.5471
	k = 7	0.5281

On the contrary, for class 1 images, the number of clusters was varied between 2 to 7 because, as explained before, the nuclei in this type of cells was smaller and belonged to

many different gray levels. Hence, separating the image in more regions made it more likely to separate nuclei from the rest of the regions.

Table 7. Jaccard index obtained when varying the radius of the structuring element, using the best result of kmeans in class 2 images and applying the morphological operations.

Method	Radius of the structuring element (disk)	Jaccard
K-means	k = 6	0.5471
Erosion	r = 1	0.4741
	r = 2	0.3887
	r = 3	0.3031
Dilation	r = 1	0.5525
	r = 2	0.5156
	r = 3	0.4616
Closure	r = 1	0.5484
	r = 2	0.5484
	r = 3	0.5458
Opening	r = 1	0.5443
	r = 2	0.5281
	r = 3	0.4992

Table 8. Jaccard indexes obtained using watersheds in class 2 images.

Method	Parameter	Jaccard
Watershed	h = 30	0.0234
	h = 45	0.2007
	h = 50	0.2975

For class 2, closure had the best performance followed by opening. This meant that some regions needed to be connected as well as some noise pixels needed to be removed.

Finally, after all variations, the best nuclei cell segmentation achieved in class 2 images resulted in a Jaccard index of 0.5484 and is shown in Figure 8.

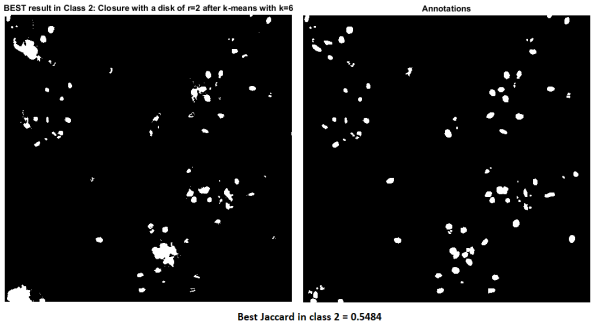

Figure 8. Best nuclei segmentation in class 2 images.

5.3. Further work

Morphological operations had good results on the class 1 images. However, the results were not as good for the class 2. Then, in order to improve both methods, supervised training of neuronal network or SVM's can provide a better performance for the class 2 images and improve even more the results obtained for class 1. Finally, a neural network can guarantee a classifier that consider the size and form of the nuclei for the different classes which facilitates their segmentation.

References

[1] J. Arz, P. Sanders, J. Stegmaier, and R. Mikut. 3d cell nuclei segmentation with balanced graph partitioning. *arXiv preprint arXiv:1702.05413*, 2017.

[2] D. N. Cells. Data Science Bowl 2018. data science bowl 2018, 2018.

[3] A. E. Charpenter. In *2018 Data Science Bowl: Technical overview*, 2018.

[4] J. A. Cottrell, T. J. R. Hughes, and Y. Bazilevs. *Isogeometric Analysis: Toward Integration of CAD and FEA*. John Wiley & Sons, New York, 2009.

[5] Y. Cui, G. Zhang, Z. Liu, Z. Xiong, and J. Hu. A deep learning algorithm for one-step contour aware nuclei segmentation of histopathological images. *arXiv preprint arXiv:1803.02786*, 2018.

[6] D. Hearn and M. Baker. *Computer Graphics*. Prentice-Hall., Englewood Cliffs, NJ, 1994.

[7] H. Irshad, A. Veillard, L. Roux, and D. Racoceanu. Methods for nuclei detection, segmentation, and classification in digital histopathology: a reviewcurrent status and future potential. *IEEE reviews in biomedical engineering*, 7:97–114, 2014.

[8] C. Jung and C. Kim. Impact of the accuracy of automatic segmentation of cell nuclei clusters on classification of thyroid follicular lesions. *Cytometry Part A*, 85(8):709–718, 2014.

[9] Kaggle. 2018 data science bowl¿ find the nuclei in divergent images to advance medical discovery, jan 2018.

[10] H. Kong, H. C. Akakin, and S. E. Sarma. A generalized laplacian of gaussian filter for blob detection and its applications. *IEEE transactions on cybernetics*, 43(6):1719–1733, 2013.

[11] C. Liu, F. Shang, J. A. Ozolek, and G. K. Rohde. Detecting and segmenting cell nuclei in two-dimensional microscopy images. *Journal of pathology informatics*, 7, 2016.

[12] T. R. C. of Pathologists of Australasia. *Pathology? the facts*. RCPA.

[13] L. Piegl and W. Tiller. *The NURBS Book*. Monographs in Visual Commu- nication, 1995.

[14] F. Raimondo, M. A. Gavrielides, G. Karayannopoulou, K. Lyroudia, I. Pitas, and I. Kostopoulos. Automated evaluation of her-2/neu status in breast tissue from fluorescent in situ hybridization images. *IEEE Transactions on Image Processing*, 14(9):1288–1299, 2005.

[15] A. Robb. What is the function of the nucleus in eukaryotic cells? In *Definition of a Eukaryote*.

[16] J. C. Simo and T. J. R. Hughes. *Computational Inelasticity*. Springer-Verlag, New York, 1998.

[17] C. Wählby, I.-M. SINTORN, F. Erlandsson, G. Borgefors, and E. Bengtsson. Combining intensity, edge and shape information for 2d and 3d segmentation of cell nuclei in tissue sections. *Journal of microscopy*, 215(1):67–76, 2004.

[18] F. Xing and L. Yang. Robust nucleus/cell detection and segmentation in digital pathology and microscopy images: a comprehensive review. *IEEE reviews in biomedical engineering*, 9:234–263, 2016.

[19] F. Xing and L. Yang. Robust nucleus/cell detection and segmentation in digital pathology and microscopy images: a comprehensive review. *IEEE reviews in biomedical engineering*, 9:234–263, 2016.